

Electronic Structure from Polarised Neutron Diffraction*

G. S. Chandler, D. Jayatilaka and S. K. Wolff

Department of Chemistry, University of Western Australia,
Nedlands, WA 6907, Australia.

Abstract

The polarised neutron diffraction experiment is described and the nature of the information obtained is outlined. In many cases interpretation of the experiment assumes that the crystal is made up of non-interacting molecular or ionic units. The soundness of this assumption is examined in the case of copper Tutton salt. Polarised neutrons are scattered by the crystal magnetisation density which has a contribution from the orbital motion of electrons. A method for including the spin-orbit contribution to this effect is described for the particular example of the CoCl_4^{2-} ion.

1. Introduction

The motivation for the work described in this paper is the drive to understand the nature of bonding in transition metal complexes. Early thinking about the matter recognised that electrons which were not already involved in bonding on a ligand could be accepted by empty sites on the metal ion, and so the concept of a coordinate covalent bond, where both the electrons involved in a bond are donated by one of the atoms in the bond was born. Of course electrons are indistinguishable, and so whether the electrons come from one atom or another is not a meaningful question to ask. However, donation from one atom to another will lead to considerable ionic character. For example, recent theoretical studies, illustrated by the interesting work of Rosi and Bauschlicher (1989, 1990), interpret bonding in transition metal–water interactions as being electrostatic in character, with the major electronic involvement being the reorganisation of the electrons on the metal to minimise repulsion between the d-electrons of the metal ion and the lone pairs of the water molecule. There can be some covalent involvement however, and various pieces of evidence indicate that the covalent character of any bonding depends on the nature of the ligand involved. The determination of the extent of covalency is of some interest and it is a factor which can be probed by polarised neutron diffraction.

Most of the understanding developed about chemical bonding has come from thermochemical and spectroscopic studies, both of which are concerned with

* Refereed paper based on a contribution to the Advanced Workshop on Atomic and Molecular Physics, held at the Australian National University, Canberra, in February 1995.

the energetics of systems. Studies of this kind are complemented by theoretical chemistry which by concentrating on energetics has contributed a great deal to our understanding of binding in small molecules from the early part of the periodic table. But transition metal complexes are difficult systems for theory, because the number of electrons is large. Energetics and theory, though, are not the only way of approaching questions of chemical bonding. Information is also available from diffraction measurements. These give information about the distribution of electrons in molecules in the form of the charge and spin density, the latter of which maps the distribution of unpaired electrons. These distributions demand different information from a wavefunction than the energy which, because of the variation theorem, the wavefunction is tailored to give best. It is believed though that good wavefunctions, in terms of the variation theorem, are also accurate in terms of the three-dimensional distribution of electrons.

Two types of diffraction are used to obtain electron distributions. X-rays are used to probe charge densities while in the right cases polarised neutrons directly give spin densities. This paper is primarily concerned with spin densities from the polarised neutron experiment, although there is an excursion into charge densities to illustrate an important point.

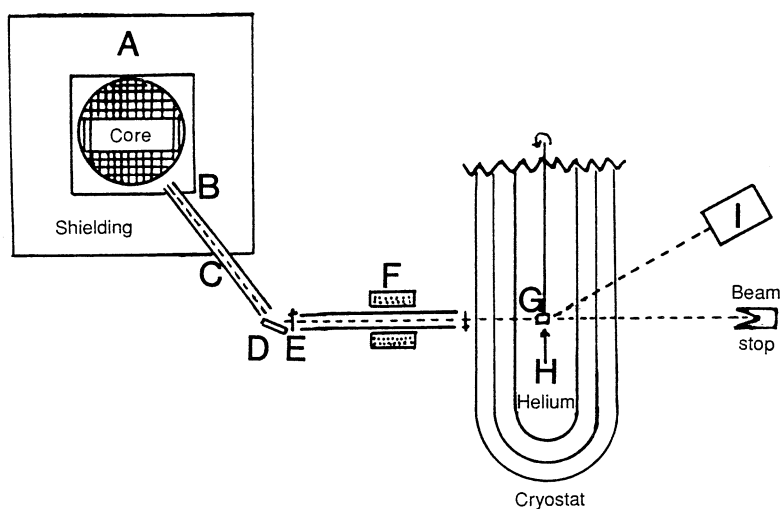


Fig. 1. Experimental set up for the polarised neutron diffraction experiment.

The polarised neutron experiment is uncommon and can only be carried out at a few locations, the major one being the Institut Laue-Langevin at Grenoble. The possibilities are exemplified in the work of Figgis, Reynolds and coworkers (1993*a, b, c*). The following brief description of the polarised neutron experiment follows that of Figgis (1990) and is summarised in Fig. 1. A nuclear reactor designed to produce a high flux of neutrons is the essential requirement. The neutrons are moderated at A, taken by a beam guide at B-C, and are made monochromatic and polarised by diffraction from a magnetised iron crystal, so that their spin is in a particular direction ('up') at D and E. The direction of polarisation can be reversed by the flipper at F. Once polarised the monochromatic beam

must travel in a magnetic field to maintain the polarisation. The sample at G, held at ~ 4 K and in a magnetic field with $H \sim 5$ T diffracts the neutrons into the Bragg directions. From the point of view of obtaining spin densities, the important point is that the scattering intensity depends on the magnetic properties of the sample and depends on whether the neutron polarisation is 'up' or 'down'. Experimentally, what is recorded are the flipping ratios—the ratio of the cross section for spin 'up' neutrons to that for spin 'down' neutrons. The flipping ratios can be manipulated to produce magnetic structure factors for Bragg reflections which are analogous to the familiar X-ray structure factors.

Analysis of the magnetic structure factors either by Fourier transformation or by least squares fitting of flexible models produces maps of the distribution of spin density in the molecule. The spin map gives direct information about the distribution of valence electrons on the metal since, in the ground state, only the valence electrons will have unpaired spin.

Theoretically, spin density distribution maps can be calculated very simply once a wavefunction is obtained. This is made clear by writing densities in terms of the densities of spin-up ρ_{\uparrow} and spin-down ρ_{\downarrow} electrons:

$$\rho_{\text{spin}} = \rho_{\uparrow} - \rho_{\downarrow}, \quad \rho_{\text{charge}} = \rho_{\uparrow} + \rho_{\downarrow}. \quad (1)$$

Spin and charge densities can be used as a point of comparison with experiment. It is, however, preferable to make comparisons with the structure factors since this avoids uncertainties which enter with the analysis of the data. Within certain approximations both magnetic and X-ray structure factors can be obtained theoretically. We have developed analytic methods for obtaining structure factors from molecular wavefunctions which are expanded in terms of atom centred Gaussian functions. This capability has led to useful interaction with experimentalists some of which are described below.

2. Theory of the Polarised Neutron Experiment

The scattering cross section for the interaction of the neutron with a crystal is given by the square of the scattering amplitude:

$$\frac{d\sigma}{d\Omega} = |F(\mathbf{k}_0, \mathbf{k})|^2, \quad (2)$$

where \mathbf{k}_0, \mathbf{k} are the propagation vectors of the incident and scattered neutron respectively. The scattering amplitude is given in the first Born approximation by

$$F(\mathbf{k}_0, \mathbf{k}) = -\frac{M_n}{2\pi\hbar^2} \int \psi^* \mathbf{V}(\mathbf{r}) \psi_0 \, d\mathbf{r}, \quad (3)$$

where M_n is the mass of the neutron, $\mathbf{V}(\mathbf{r})$ is the potential of the neutron in the magnetic field created within the crystal, and $\psi_0 = \chi_0 \exp(i\mathbf{k}_0 \cdot \mathbf{r})$ and $\psi = \chi \exp(i\mathbf{k} \cdot \mathbf{r})$ are wavefunctions for the incident and scattered neutron respectively.

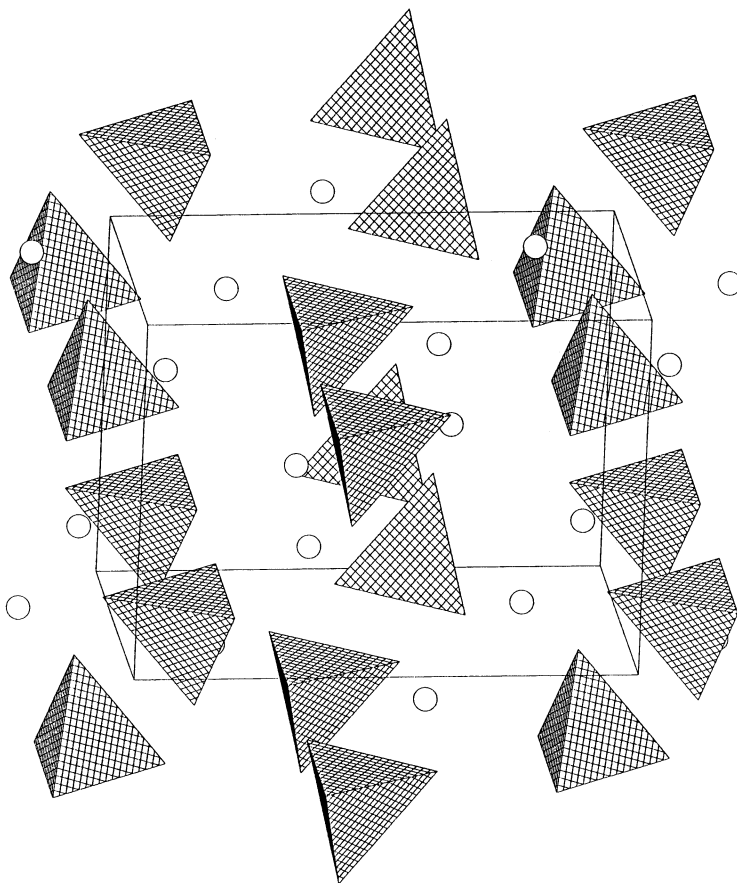


Fig. 2. The crystal structure of Cs_2CoCl_4 .

To make progress in calculating scattering amplitudes it is necessary to compute $V(\mathbf{r})$. In the majority of transition metal compounds which have been studied experimentally, the crystal consists of ionic units which are sufficiently separated for them to be considered as non-interacting units. An example is caesium tetrachlorocobaltate (Cs_2CoCl_4). A diagrammatic representation is shown in Fig. 2. The circles represent Cs^+ ions. The tetrahedra are CoCl_4^{2-} units in which four Cl^- ions are bound to the cobalt with Co-Cl distances of about 226 pm. This tetrahedral array constitutes one ionic unit, the other is the Cs^+ ion. Atoms within each tetrahedral CoCl_4^{2-} unit are considerably closer to each other than they are to any other ions in the structure. As a consequence, for crystals of this type, the crystal potential can be written in terms of a sum over the potentials for each ion in the unit cell convoluted over the lattice density $L(\mathbf{r})$:

$$V_{\text{crystal}}(\mathbf{r}) = \left(\sum_j V_{\text{mol},j}(\mathbf{r} - \mathbf{r}_j) \right) * L(\mathbf{r}). \quad (4)$$

This assumption is similar to that made for structure determinations with X-rays, but in that case, the summation is over atoms rather than ionic fragments. The

molecular potential is given by

$$V_{\text{mol},j}(\mathbf{r}) = \frac{2\pi\hbar^2}{M_n} \sum_k T_{jk} b_{jk} \delta(\mathbf{r} - \mathbf{r}_j - \mathbf{r}_{jk}) - 2\gamma\mu_N \mathbf{S} \cdot \mathbf{B}_j(\mathbf{r}), \quad (5)$$

with $T_{jk} = \exp[-\frac{1}{2}\mathbf{q}^t \Lambda_{jk} \mathbf{q}]$. In (5), b_{jk} is the experimental scattering length, γ the magnetic moment of the neutron in nuclear magnetons, μ_N the nuclear magneton, \mathbf{S} the spin of the neutron, \mathbf{B}_j the thermally averaged magnetic flux of the molecule, \mathbf{q} the scattering vector $\mathbf{k}_0 - \mathbf{k}$ and Λ_{jk} is the experimentally determined thermal tensor for nucleus k in molecule j .

The first term of (5) takes account of scattering from the individual nuclei labelled k . The second term is the interaction energy between the spin of the neutron and the thermally averaged magnetic flux arising from molecule j . This results from spin density and electron currents from the orbital motion of the electrons. Putting (5) into (3) gives an expression for the scattering amplitude involving the Fourier transform of the magnetic flux within the unit cell. This expression will be discussed in a later section. At this stage though, it is convenient to examine the assumption inherent in obtaining (4), that the ions in the crystal can be treated as being non-interacting. This examination has been accomplished by determining the X-ray structure factors of copper Tutton salt, $(\text{ND}_4)_2\text{Cu}(\text{SO}_4)_2 \cdot 6\text{D}_2\text{O}$.

3. X-ray Structure Factors for $(\text{ND}_4)_2\text{Cu}(\text{SO}_4)_2 \cdot 6\text{D}_2\text{O}$

Accurate Bragg intensities for $(\text{ND}_4)_2\text{Cu}(\text{SO}_4)_2 \cdot 6\text{D}_2\text{O}$ at 9 K are available from the work of Figgis *et al.* (1993a). In order to test the assumption of non-interacting ions it is necessary to consider the familiar general expression for the structure factor for a crystal

$$F(\mathbf{q}) = \sum_j^N \exp(i\mathbf{q} \cdot \mathbf{r}_j) \tilde{\rho}_j, \quad (6)$$

where \mathbf{q} is the scattering vector, \mathbf{r}_j the position vector for the ion and $\tilde{\rho}_j$ the Fourier transform of the thermally averaged molecular charge density. While this expression containing the charge density is familiar for X-ray diffraction, ρ_j could equally well be a spin density or current density in which case (6) would represent the general form of the structure factor derived from (5) and (3) and be applicable to polarised neutron diffraction. In calculating the structure factors for this situation the computational problem is to evaluate (6) with $\tilde{\rho}_j$ derived from molecular wavefunctions.

For most cases there will be more than one ion of each type per unit cell. In general these ions will be oriented differently in the unit cell. The wavefunctions of these rotated ions are related by a unitary transformation \mathbf{U} . Thus the wavefunction at k is related to that at j by

$$\psi_k(\mathbf{r}) = \psi_j(\mathbf{U}^t \mathbf{r}). \quad (7)$$

Thus the contribution of each ion to the scattering factor can be simply included by making the appropriate unitary transformation to the wavefunction for each ion.

A further computational task is to account for thermal smearing since experiment produces thermally smeared structure factors. In our work thermal smearing is handled by partitioning molecular densities into atomic and overlap densities using the Mulliken (1955) scheme. From this partitioning, mean atomic densities are obtained by convoluting the static atomic densities with the experimentally obtained thermal tensors for the respective atoms. What remains is the question of dealing with the overlap densities. Previous work has suggested the use of a combination of the thermal tensors of the two atoms joined in the bond which produces the overlap density (Coppens *et al.* 1971; Stewart 1969). Thus if two atoms A and B are bound with thermal tensors Λ_A and Λ_B and C is centrally between them and considered to be the centre of the overlap density, then two expressions have been proposed for Λ_C —one by (Coppens *et al.* 1971),

$$\exp(-\frac{1}{2}\mathbf{q}^t\Lambda_c\mathbf{q}) = \frac{1}{2}[\exp(-\frac{1}{2}\mathbf{q}^t\Lambda_A\mathbf{q}) + \exp(-\frac{1}{2}\mathbf{q}^t\Lambda_B\mathbf{q})]. \quad (8)$$

and one by (Stewart 1969)

$$\exp(-\frac{1}{2}\mathbf{q}^t\Lambda_c\mathbf{q}) = \exp[-\frac{1}{4}\mathbf{q}^t(\Lambda_A + \Lambda_B)\mathbf{q}]. \quad (9)$$

In practice both (8) and (9) give very similar structure factors.

The major task in the evaluation of (6) is calculating the Fourier transform of ρ_j . Since the majority of molecular wavefunctions are expanded in terms of Gaussian-type orbitals we have written a programme to obtain both conventional and magnetic structure factors from Gaussian-type wavefunctions. At the heart of the programme is the Fourier transform of the product of Gaussian functions which appear in the density expressions ρ_j . The transformations are accomplished analytically using a generalisation of the expressions published by Chandler and Spackman (1978). Given a Gaussian function centred at A,

$$G_A(A, \alpha_A, l, m, n) = N_A(x - r_{A,x})^l(y - r_{A,y})^m(z - r_{A,z})^n \exp(-\alpha_A|\mathbf{r} - \mathbf{r}_A|^2), \quad (10)$$

it can be shown that

$$\begin{aligned} \int x^l y^m z^n G_A G_B \exp(i\mathbf{q} \cdot \mathbf{r}) \, d\mathbf{r} &= N_A N_B (\pi/\rho)^{3/2} \exp\left(\frac{Q^2}{\rho} - \alpha_A \mathbf{r}_A^2 - \alpha_B \mathbf{r}_B^2\right) \\ &\times \sum_{i=0}^{l_1+l_2} f_i(l_1, l_2 - r_{A,x}, -r_{B,x}) g_{i+l}(p, Q_x) \\ &\times \sum_{j=0}^{m_1+m_2} f_j(m_1, m_2 - r_{A,y}, -r_{B,y}) g_{j+m}(p, Q_y) \\ &\times \sum_{k=0}^{n_1+n_2} f_k(n_1, n_2 - r_{A,z}, -r_{B,z}) g_{k+n}(p, Q_z), \end{aligned} \quad (11)$$

with

$$p = \alpha_A + \alpha_B, \quad \mathbf{Q} = \alpha_A \mathbf{r}_A + \alpha_B \mathbf{r}_B + \frac{1}{2} i \mathbf{q},$$

$$g_n(p, Q_x) = n! \left(\frac{Q_x}{p} \right)^{n[n/2]} \sum_{k=0}^{n[n/2]} \frac{1}{(n-2k)! k!} \left(\frac{p}{4Q_x^2} \right)^k,$$

$$f_j(l, m, a, b) = \sum_{i=\max(0, j-m)}^{i=\min(j, l)} \binom{l}{i} \binom{m}{j-i} a^{l-i} b^{m+i-1-j},$$

where $[n/2]$ is the largest integer less than or equal to $n/2$.

With a programme incorporating the features outlined above (6) can be evaluated for copper Tutton salt. Three models were examined for the calculation of structure factors: (1) a non-interacting atom model; (2) a non-interacting molecule model and (3) an empirical model in which $F(\mathbf{q})$ were calculated from a multipole fit to the experimental $F(\mathbf{q})$.

For the molecular and atomic calculations a variety of basis sets were used ranging from single zeta to basis sets which are triple zeta for the valence functions and with polarisation functions added to the largest sets in the case of molecules. The basis sets were used in restricted Hartree-Fock calculations on the closed shell ions and in unrestricted Hartree-Fock calculations for the open shell $[\text{Cu}(\text{H}_2\text{O})_6]^{2+}$ ion. Geometries used come from the neutron structure (Figgis *et al.* 1993a). Thermal parameters were taken from the *neutron* diffraction experiment at 9 K.

The various models are evaluated by comparing a set of calculated structure factors with those obtained experimentally. The measure of comparison used is χ^2 , defined as

$$\chi^2 = \frac{1}{N} \sum_i (F_{ci} - F_{0i})^2 / \sigma_{0i}^2, \quad (12)$$

where N is the number of structure factors being compared, F_c is the calculated structure factor, F_0 is the experimental structure factor and σ_{0i}^2 is the experimental standard error. A full discussion of this study can be found in Chandler *et al.* (1994). Here the principal results are shown in a series of figures.

Fig. 3 is a plot of χ^2 for a particular calculation versus the number of basic functions per unit cell used in the calculation. The behaviour of χ^2 suggests that for structure factors the basis set is approaching a limit.

Fig. 4 illustrates the importance of thermal motion even at 9 K. Fig. 4a shows χ^2 versus $\sin\theta/\lambda$ for $F(\mathbf{q})$ without thermal smearing; the basis set is large. Fig. 4b shows the effect of including thermal smearing. If the different scales for χ^2 are noted the extreme importance of including thermal motion is immediately apparent. Also of interest is the fact that the charge density is not uniformly sampled by $\sin\theta/\lambda$. High values of $\sin\theta/\lambda$ are dominated by the core density, whereas valence density predominates in the low angle scattering. Bearing this in mind, it is evident from Fig. 4b that, when temperature factors

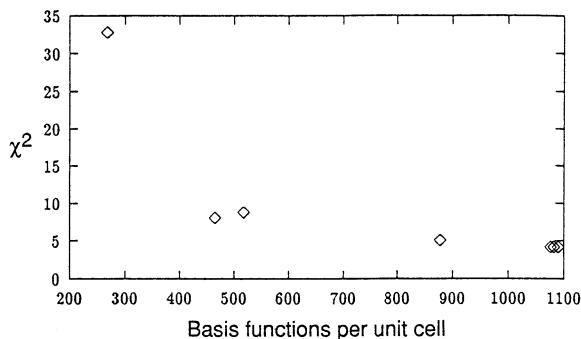


Fig. 3. Plot of χ^2 versus the number of basis functions per unit cell.

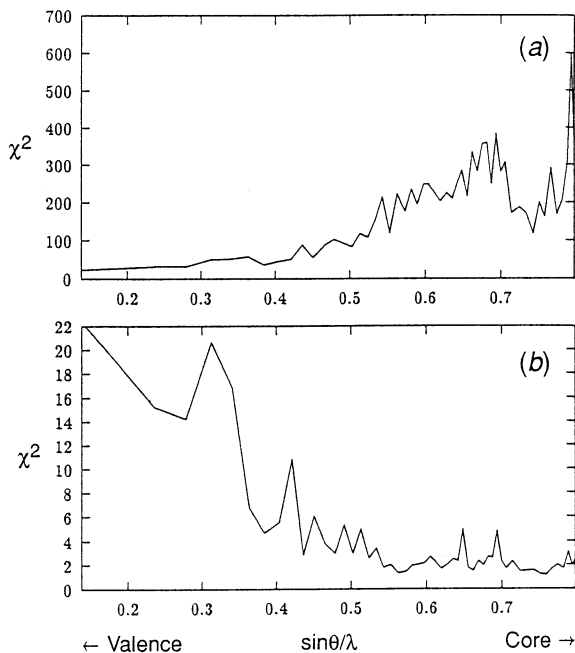


Fig. 4. Plot of χ^2 versus $\sin\theta/\lambda$ for (a) a large basis and no thermal motion and (b) for the same basis as (a) but with thermal motion included.

are included, the structure factors not being modelled correctly are those which come predominantly from the valence electrons.

The evidence for the reasonableness of the non-interacting ion model is contained in Table 1. In this table χ^2 and conventional R factors are tabulated for the three models, with a number of basis sets shown for the ionic calculations. The independent spherical atom model (SPAT) calculated with the largest basis set used for the ions is the poorest model. The agreement from *ab initio* Hartree–Fock molecular calculations improves as the basis sets increase in size. The least satisfactory is the single zeta basis (SZ) followed in order of increasing agreement

Table 1. Agreement factors between theoretical and experimental structure factors for various theories

Theory	χ^2	$R(F)$ (%)
SPAT	40	3.52
SZ	33	2.82
DZV	7.9	1.57
DZP	5.2	1.40
TZVP	4.3	1.30
BEMP	2.7	1.14

by a basis which is double zeta in the occupied valence orbitals (DZV), one which is double zeta with polarisation functions (DZP), and the largest basis (DZTV). Details of these bases are given by Wolff *et al.* (1995). The best non-interacting molecule result is striking in that with just two parameters it gives almost as good agreement as the empirical model (BEMP) with 184 parameters used in fitting the experimental data. It is clear that we have explained, using only *ab initio* theory on isolated molecules, a large fraction of the change in electron density on formation of the crystal from its constituent ions.

Armed with the assurance that, for crystals of the type illustrated in Fig. 2, the non-interacting ion model is reasonable, we can return to a consideration of polarised neutron diffraction.

4. Polarised Neutron Diffraction Pattern of Cs_3CoCl_5

Polarised neutrons, as already pointed out, are scattered by the molecular magnetic field. For transition metal ions which are not orbitally degenerate, the magnetisation density arises, as a first approximation, from the electron spin alone. This ignores spin-orbit coupling, which allows an orbital contribution to the magnetisation. In the spin only case magnetic structure factors are scalar quantities. With an orbital contribution they become vector quantities and their transform is a magnetisation density which is no longer colinear with the applied magnetic field. The result is that there is no longer a direct association with the spin density which carries the information about bonding within the complex ions. Theoretical assessment of the magnitude of spin-orbit effects is obviously of some importance. This section outlines progress made in this respect and gives the application of the theory to diffraction in the case of the orbitally non-degenerate Cs_3CoCl_5 molecule.

To achieve this aim it is convenient to develop a different form for the structure factors from that given in (6). After some algebra (2) can be converted to the following expression for the scattering cross section for polarised neutrons from centrosymmetric crystals:

$$(|\mathbf{F}_N + \vartheta \mathbf{P}_0 \cdot \mathbf{F}^\perp|^2 + \vartheta^2 |\mathbf{P}_0 \times \mathbf{F}^\perp|^2) \frac{(2\pi)^3}{V_{\text{cell}}} \sum_m \delta(\mathbf{q} - 2\pi \mathbf{D}^* \mathbf{m}), \quad (13)$$

where \mathbf{m} are the Miller indices for the reciprocal lattice vector, \mathbf{D}^* is a matrix whose columns are the reciprocal lattice vectors, ϑ is a constant and \mathbf{P}_0 is the neutron polarisation vector.

In (13) the molecular contributions appear in \mathbf{F}_N which is the nuclear contribution to scattering and \mathbf{F}^\perp , the magnetic structure factor, which is the magnetic part of the molecular contribution. Expanding \mathbf{F}^\perp gives

$$\mathbf{F}^\perp(\mathbf{q}) = \left(\frac{c^2}{8\pi\mu_B} \right) \sum_j \exp(i\mathbf{q} \cdot \mathbf{r}_j) 2\tilde{\mathbf{B}}_j(\mathbf{q}). \quad (14)$$

Previous work has developed this expression in terms of the magnetisation density (magnetic moment per unit volume). This formulation has proved to be intractable for molecules without using approximations. Instead we have expressed it in terms of $\tilde{\mathbf{J}}$ the Fourier transform of the current density, which is easy to visualise since the movement of charge will give rise to a magnetic field. In this form

$$\mathbf{F}^\perp(\mathbf{q}) = - \left(\frac{i}{2\mu_B \kappa_c q^2} \right) \sum_j \exp(i\mathbf{q} \cdot \mathbf{r}_j) \mathbf{q} \times \tilde{\mathbf{J}}_j(\mathbf{q}), \quad (15)$$

where \mathbf{J} itself can be decomposed into a sum of contributions

$$\mathbf{J}(\mathbf{r}) = \mathbf{J}_L(\mathbf{r}) + \mathbf{J}_S(\mathbf{r}) + \mathbf{J}_{\text{dia}}(\mathbf{r}). \quad (16)$$

Here \mathbf{J}_L is the orbital contribution, which is necessarily zero if there is no orbital angular momentum when the wavefunction is real. Also \mathbf{J}_S is the contribution from the net spin of the electrons. Lastly, there is the small diamagnetic contribution present in all molecules. In this form, analytic expressions for the magnetic structure factors can be obtained. They are readily evaluated from molecular wavefunctions using the computational scheme outlined in Section 3.

To demonstrate the viability of these procedures we have calculated magnetic structure factors which include spin-orbit coupling effects for CoCl_4^{2-} as found in the crystalline environment of Cs_3CoCl_5 . The CoCl_4^{2-} ion has a ${}^4\text{B}_1$ ground state (Barnes *et al.* 1989) and so has no orbital angular momentum. However, spin-orbit coupling allows the mixing in of states which have orbital angular momentum giving a wavefunction for which \mathbf{J}_L of (16) is not zero. To obtain the wavefunction the following Hamiltonian was used

$$H = H_0 + H_B + H_{\text{SO}}, \quad (17)$$

where H_0 is the usual Hamiltonian of quantum chemistry

$$H_0 = - \frac{\hbar^2}{2m_e} \sum_i \nabla_i^2 - \frac{e^2}{4\pi\epsilon_0} \sum_{i,n} \frac{Z_n}{r_{ni}} + \frac{e^2}{8\pi\epsilon_0} \sum_{i \neq j} \frac{1}{r_{ij}}, \quad (18)$$

H_B includes the interaction with an external magnetic field \mathbf{B}

$$H_B = -i\mu_B \sum_i \mathbf{B} \cdot [\mathbf{r}_i \times \nabla_i] + g_e \mu_B \sum_i \mathbf{B} \cdot \mathbf{S}_i + \frac{e^2}{8m} \sum_i |\mathbf{B} \times \mathbf{r}_i|^2, \quad (19)$$

and where $\mu_B = |e|\hbar/2m_e$. The spin-orbit interaction is included with H_{SO} :

$$H_{SO} = i \frac{g_e \mu_B^2}{4\pi\epsilon_0 c^2} \sum_{n,i} \frac{Z_n}{r_{ni}^3} \mathbf{S}_i \cdot [\mathbf{r}_{ni} \times \nabla_i] + \frac{g_e \mu_B^2 |e|}{8\pi\epsilon_0 \hbar c^2} \sum_{n,i} \frac{Z_n}{r_{ni}^3} \mathbf{S}_i \cdot [\mathbf{r}_{ni} \times (\mathbf{B} \times \mathbf{r}_i)]. \quad (20)$$

The vector $\mathbf{r}_{ni} = \mathbf{r}_i - \mathbf{R}_n$ is the difference between the position of an electron and a nucleus.

Single determinantal solutions to the Hamiltonian were obtained using the unrestricted Hartree-Fock formalism. In order to accommodate the mixing of spin functions $|\alpha\rangle$ and $|\beta\rangle$ caused by the external magnetic field and spin-orbit interaction, the orthogonal molecular spin-orbitals ϕ_p were expressed as a linear combination of spin-space product basis functions in the following way:

$$\begin{aligned} \phi_p &= \phi_p^\alpha |\alpha\rangle + \phi_p^\beta |\beta\rangle, \\ \phi_p^\alpha &= \sum_\mu C_{\mu p}^\alpha \chi_\mu, \quad \phi_p^\beta = \sum_\mu C_{\mu p}^\beta \chi_\mu. \end{aligned} \quad (21)$$

Details of these calculations and the subsequent discussion can be found in Wolff *et al.* (1995).

What effect does the spin-orbit interaction have on the agreement with experiment? This is summarised in Fig. 5. The calculations employed a variety of basis sets. Agreement in this instance is measured in terms of a scale factor g . This is the factor which when applied to all calculated structure factors minimises χ^2 in equation (12). Fig. 5 has $1/g$ plotted on the ordinate. A value of $1/g < 1$ means that on average the magnitudes of the structure factors are too low, a value greater than one means they are too high. It is clear that, for all basis sets, the spin only structure factors are too low, both with and without the inclusion of thermal smearing. There is a considerable change upon including the spin-orbit interaction through (17). The structure factors are now too high and the inclusion of thermal smearing improves the agreement with experiment rather than worsening it as happens in the other case. Agreement between experiment and theory is still not impressive. However, the Hamiltonian (17) does not include the two-electron terms which would have the effect of shielding the electrons from the nucleus ($Z = 27$). That this indeed would have an appreciable effect has been tested by using an effective nuclear charge of 9 for the d-orbitals. This is the effective charge obtained using Slater's rules. The points from this correction are the open diamond and triangle in Fig. 5; the latter includes thermal smearing. This is a substantial improvement in agreement with experiment.

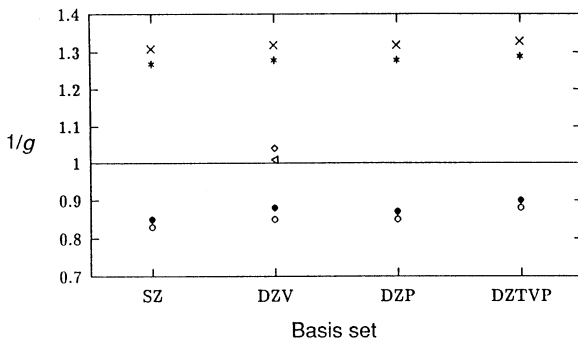


Fig. 5. The $1/g$ scale factor for magnetic F_M and spin-only F_{S_z} structure factors: F_{S_z} (no thermal motion) = ●; $F_{S_z} = 0$; F_M (no thermal motion) = ×; $F_M = *$; F_M (no thermal motion) from an effective $Z = 9 = \diamond$; F_M from an effective $Z = 9 = \triangle$.

5. Conclusion

Even though the application of polarised neutron diffraction is still in its infancy, it has been shown to be capable of revealing important information about bonding in transition metal complexes, especially about the extent of covalent interactions. So far experiments have been mostly confined to centrosymmetric structures. However, sizeable molecules can be handled, much larger than computational chemistry can treat with any sort of rigour. Nevertheless, computation can deal with small archetypal systems and gives valuable insights to aid the interpretation of experiment.

References

- Barnes, L. A., Chandler, G. S., and Figgis, B. N. (1989). *Mol. Phys.* **68**, 711.
 Chandler, G. S., and Spackman, M. A. (1978). *Acta Cryst. A* **34**, 341.
 Chandler, G. S., Figgis, B. N., Reynolds, P. A., and Wolff, S. K. (1994). *Chem. Phys. Lett.* **225**, 421.
 Coppens, P., Willoughby, T. V., and Csonka, L. N. (1971). *Acta Cryst. A* **27**, 248.
 Figgis, B. N. (1990). *Proc. Ind. Acad. Sci.* **102**, 403.
 Figgis, B. N., Iversen, B. B., Larsen, F. K., and Reynolds, P. A. (1993a). *Acta Cryst. B* **49**, 794.
 Figgis, B. N., Kucharski, E. S., and Vrtis, M. (1993b). *J. Am. Chem. Soc.* **115**, 176.
 Figgis, B. N., Reynolds, P. A., and Cable, J. W. (1993c). *J. Chem. Phys.* **98**, 7743.
 Mulliken, R. S. (1955). *J. Chem. Phys.* **23**, 1833; **23**, 1841.
 Stewart, R. F. (1969). *J. Chem. Phys.* **51**, 4569.
 Rosi, M., and Bauschlicher, C. W., Jr (1989). *J. Chem. Phys.* **90**, 7264.
 Rosi, M., and Bauschlicher, C. W., Jr (1990). *J. Chem. Phys.* **92**, 1876.
 Wolff, S. K., Jayatilaka, D., and Chandler, G. S. (1995) *J. Chem. Phys.* **103**, 4562.